Toward the use of single crystal diamond based detector for ion-beam therapy microdosimetry.

C.Verona[1*], G. Magrin[2], P. Solevi[3], M. Bandorf[2,3], M. Marinelli[1], M. Stock[2] and G. Verona Rinati[1]

[1] *INFN - Dipartimento di Ingegneria Industriale, Università di Roma "Tor Vergata", via del Politecnico 1, Roma 00133, Italia*

[2] *EBG MedAustron Marie Curie-St. 5, 2700, Wiener Neustadt, Austria*

[3]*Institut für Medizintechnik, Otto-von-Guericke Universität, Magdeburg, Germany*

Abstract

In this work, the fabrication and characterization of a microdosimeter based on a synthetic single crystal diamond is reported. The microdosimeter is realized by means of both standard photolithography and selective chemical vapor deposition techniques to accurately define its micrometric sensitive volume.
Experimental measurements were carried out at the Ruđer Bošković Institute microbeam facility using different particles such as proton, helium, lithium, carbon and oxygen. Ion beam induced charge (IBIC) technique was performed to characterize the microdosimeter response in terms of its charge collection properties. The experimental data were also analyzed by means of Geant4 Monte Carlo simulations.
Diamond based microdosimeter shows a well-defined active volume. Homogeneity of the response was estimated of about 7% and linked to structural defects of diamond surface as deduced by AFM inspection. The detector response shows a good linear behaviors for different kind and energy ions indicating that the detector is suitable for measuring a wide range of particles and LET i.e. 100÷3000 keV/µm. Finally, microdosimetric capabilities of the diamond based microdosimeter were preliminarily tested in low LET radiation fields (i.e. protons beam).

1. Introduction

Diamond has been identified as a desirable material for use in microdosimetry due to its near tissue equivalence (its atomic number, Z=6, is very close to the atomic number of a biological tissue, Z= 7.5) and radiation hardness [1-3]. In particular, theoretical study [4] demonstrated that it is possible to convert the energy deposited in diamond to water for protons beam by using an appropriate correction factor so that diamond can be considered as tissue equivalent for protons in addition to photons and electron beams.
A microdosimeter should be able to measure the distribution of imparted energies in targets of micrometric sizes exposed to complex radiation fields, providing the information that, together with absorbed dose, relates to radiobiological effects (RBE) of ionizing radiation [5,6]. Microdosimeters based on chemical vapor deposition (CVD) single-crystal diamond have been recently proposed in the literature [7-10] for ion-beam therapy applications. In particular, diamond based Schottky diodes have been fabricated and tested in the framework of a collaboration between "Tor Vergata" University and

EBG MedAustron [10,11] to assess their possible use during the phases of commissioning of the ion beams and the clinical periodic routines. These detectors exhibit several advantages such as zero bias voltage operation, small dimension, good spectroscopic properties (i.e. charge collection efficiency close to 100% and good energy resolution) and high radiation tolerance [4].
Such devices could be useful for other radiation therapy applications too. Targeted alpha-radionuclide therapy (TAT) employs radiopharmaceuticals labelled with alpha-emitters to deliver high dose to tumor cells with high specificity [12]. Many radiopharmaceuticals for TAT are currently undergoing different phase trials, however their clinical implementation would definitely benefit from a better understanding of the RBE for different cell lines and end-points. The micro-metric thickness of the sensitive region of diamond detector compared to the short range of alpha particles, could improve the characterization of the RBE.
Moreover, the miniaturization and easy-stable operational use of diamond detectors make them suitable for the inclusion in catheters with the purpose of monitoring the dose released to reference points during either external radiotherapy treatments or, more interesting, during brachitherapy applications. High Dose Rate (HDR) brachitherapy is based on the possibility to deliver dose to any target tumor that could be accessed by a catheter or applicator [13]. Despite the placement of the catheters is performed under image-guidance, the integration of real-time detectors could provide in-vivo verification of the delivered dose thus benefiting the outcome of the treatment.
Several optimizations on the diamond detector were lately achieved. In particular, the transversal definition of diamond sensitive volume has been improved and the welding material was displaced from the part which defines the sensitive volume of the detector. In other case, the welding material would behave as an absorber degrading the energy of ions which cross the sensitive volume and consequently distorting the spectra of the signal of energy deposition, depending on the particle type and energy. This effect is appreciable in the IBIC map reported in reference 6 and 9.
In this paper, a novel design of diamond based microdosimeter is presented and all the regions of the detector have been characterized in terms of the possible contributions to the charge collection signal. To this purpose, the detector has been characterized by using Ion Beam Induced Charge (IBIC) technique, available at the Ruđer Bošković Institute (RBI) ion microprobe facility. The diamond prototype has been tested with different ions of energies of a few mega electron volts, which are significant in particular for ion beam therapy applications. Finally, the experimental results have been also analyzed in terms of Monte Carlo simulations.

2. Materials and Methods

2.1.Diamond based microdosimeter

The diamond based microdosimeter (DBM from now) has a multilayered structure obtained by a two-step growing procedure by Microwave Plasma Enhanced CVD (MWPECVD) technique. Selective CVD deposition of diamond has been adopted in order to accurately define the detector geometry.
The fabrication process consists on the following steps. First, a chromium layer of 300 nm in thickness is thermally evaporated on a commercial, low cost, high pressure high temperature (HPHT) single

crystal diamond substrate. A first photolithography step is then performed in order to define the geometry of the back electrode (Fig.1-a). The p-type diamond is selectively grown by MWPECVD on diamond substrate by using a patterned chromium plasma-resistant mask (Fig.1-b). A sheet resistance of about 1.5 kΩ/sq was measured by Hall effect measurements at room temperature in air. The p-type diamond electrode has a square shape of 300 × 300 μm^2 in size connected by a 20 μm p-type diamond strip to a second p-type diamond bond-pad (120 μm × 120 μm in size). The chromium mask is then removed by wet chemical etching and an intrinsic diamond layer is selectively homoepitaxially grown by following the same procedure reported above (Fig.1-c and 1-d). The thickness of the intrinsic diamond layer is about 0.8±0.05 μm as measured by Atomic Force Microscope. The intrinsic diamond layer is oxidized, after the growth, by isothermal annealing at 500 °C for 1h in air, in order to remove the hydrogen surface conductive layer.

A chromium contact (50 nm thick), aligned over the p-type diamond backing contact, is patterned on the CVD intrinsic diamond surface by using a lift-off photo-lithographic technique (Fig.1-e). The chromium electrode has a square shape of 300 μm × 300 μm in size. Finally, a second chromium layer, which acts as welding pad electrode (120 μm × 120 μm in size), is realized by using a second lift-off photo-lithographic technique step (Fig.1-f). The DBM is schematically shown in Fig.1-g and a SEM image of DBM is reported in Fig.1-h.

A 50 μm aluminum wire is then used to micro-bond the welding pad electrodes (both p-type diamond and metallic contact) in order to provide the electrical connection to the readout electronics.

The microdosimeter is in practice a p-i-metal structure with the metallic rectifying contact having a Schottky barrier of about 1.2 eV as deduced from previous studies [14]. In all of the tests reported in the present work, the DBM was always operated at 0 V.

In order to evaluate the device sensitive thickness, capacitance-voltage (C-V) measurements have been performed using an Agilent 4284A LCR meter. The sensitive volume of the DBM can be approximated by a parallel plate capacitor, whose depletion layer thickness W can be derived as follows: $W = \frac{\varepsilon_0 \varepsilon_r A}{C}$, where A is the active device area (300 μm × 300 μm), ε_0 is the dielectric constant of free space, ε_r (5.7) is the relative permittivity of diamond and C is the device capacitance. Fig.2 shows the C-V curve for DBM device at room temperature and at 1 kHz frequency in the ±1 V bias range with a bias step of 0.05 V. The C-V was measured by sweeping the bias from 0 V to + 1 V followed by an opposite direction sweeping. There is not significant hysteresis during the biases sweeping. Using the equation reported above, a depletion thickness of about 0.72 μm is extracted from the C-V measurements at zero bias voltage condition. Such a value tends to about 0.8 μm as the bias voltage is increased, which corresponds to the thickness of intrinsic diamond film obtained by the AFM technique.

2.1.Experimental set-up

The DBM has been characterized at the Ruđer Bošković Institute (RBI) ion microprobe facility [15]. The ions were accelerated by a 6 MV Tandem Van de Graaff accelerator. IBIC technique has been employed to characterize the detector response in terms of its charge collection properties, uniformity of the response and confinement of the sensitive volume.

The detector was placed in vacuum at the end of the beam line (with residual pressure below 10^{-5} mbar) in perpendicular position respect to the ion beam direction. Different areas of the sample were irradiated by raster scanning the microbeam on its surface. The size of irradiated areas of the detector were varied in the range from 100 μm × 100 μm up to 500 μm × 500 μm.
The calibration of the beam position and IBIC image dimension was made scanning the microbeam over a silicon diode with a copper wire mask with calibrated micrometric mesh positioned on top of it. The uncertainty of the ion position was estimated in the range 1μm÷3μm, depending on the set-up of the focusing magnets, and on the species and energy of the ions. The spot size of the focused ion beam was approximately 1 μm.
The DBM was connected to a conventional charge-sensitive electronic chain, consisting of a charge-sensitive preamplifier ORTEC 142A and an ORTEC 570 shaping amplifier. The shaping time of the amplifier was set to 0.5 μs. Pulse height spectra for the incident ions were measured using an analog to digital multichannel analyzer CAMBERRA 8075.
Different ion beams and energies were used i.e. proton, helium, lithium, carbon and oxygen. The ions employed in the experiment are reported in Table 1. The penetration depths of the different ions in diamond vary between 1.8 μm and 21 μm allowing the ions to cross the DBM sensitive region. The LET profiles of the tested ions as a function of penetration depth in diamond have been calculated by Monte Carlo simulations and reported in Fig.3. Summary data of the interaction of ions within the diamond detectors have been produced by means of the multi-purpose Monte Carlo tool Geant4 (Geant4.9.10, patch 01 version) [16, 17]. The interactions are computed according to the standard electromagnetic physics, and nuclear stopping effect is based on ICRU49 parameterization. The maximum step length within the sensitive region is set to 10 nm, to sample the energy imparted with the desired precision. The Monte Carlo returns the energy imparted to the sensitive layer per ion. The LET is then calculated by dividing the mean imparted energy by the thickness of the diamond layer. Following the Poisson statistics, the number of simulated events per ion-type yields a precision below 1%.
The gain of the shaping amplifier was adapted to the different ions and energies in order to obtain spectra which extend to the highest channels. For each gain value, a separate calibration of the electronic chain was performed generating pulses at the test input of the preamplifier with an ORTEC 419 precision pulse generator. The test pulse was formed using the minimum selectable rise time on the pulse generator (approximately 5 ns) to conform to the very fast signal generated on diamond detector by the ions. Energy calibration was performed using a 500 μm thick silicon PIN diode with known Charge Collection Efficiency (CCE) of 100%. The calibration for the diamond detector was then obtained by taking into account the mean energy needed to create an electron hole pair in silicon (3.6 eV) and in diamond (13.2 eV).
The ion fluxes used were of the order of few thousand particles per second. Beam scanning, pulse height processing, and 2D-map acquisition were carried out using the SPECTOR data acquisition software, developed at RBI [18].

3. Results and discussion

A typical IBIC map acquired by DBM is reported in upper side of Fig.4, where the full area of the sample were scanned by the Li ion beam of 14.46 MeV. A quite uniform response can be appreciated,

very well confined within the 300μm × 300μm sensitive area with straight borders. The edge broadening of the sensitive area is comparable to the size of the beam spot (about 1 μm) demonstrating a high transverse definition capability of diamond based microdosimeter as evidenced by horizontal (X) and vertical (Y) profiles of the IBIC map shown in Fig.4a. The response shows a steep reduction as the beam is outside the active volume of the detector following the decrease of the electric field with the lateral distance away from the active volume. In particular, according to a previous theoretical study [16], only particles that cross the active volume within 1 μm outside the border can contribute to a readable signal. Free carriers produced by the ionization outside the sensitive area do not induce detectable signals including those impinging on the bond-pad electrode. However, some counts recorded outside the sensitive detector area are mainly due to ions that are scattered on residual gas molecules in the beam line tubes. It is should be noticed that, the X profile of the sensitive area shows an approximately constant signal, whereas Y profile shows deviations of about 20% between the signal at the central position and that at the borders. This latter behaviour is under investigation in order to understand if it is related to the detector or originates from an artefact of the measurement.

The optical image of DBM is also reported in Fig.4b as a guide to the eye for the evaluation of the superficial electrode and wire micro-bonding position. The area of the sample near the bond-pad electrode was also scanned by the Li ion beam. None distortion of the signal in the IBIC map and no detected signal due to bond-pad electrode is present as clearly visible in Fig 4c. These findings confirm that the novel microdosimeter show a well-defined active volume with high spatial resolution and, no distortions of the detected signal due to welding material are visible. Such a spatial definition of DBM is much higher than the one reported in the literature [7,8], allowing to further optimize the device geometry for specific microdosimetric application. In particular, the high definition of the sensitive volume makes it possible to realize microdosimetric arrays with high spatial resolution.

The IBIC map displays a qualitative representation of the average charge deposited per pixel. By adapting the colour temperature, it is possible to emphasize the pattern of the charge collection efficiency in different regions of the IBIC map. Thin parallel stripes characterized by lower CCE are visible in the IBIC map. Such structures are better visible in Fig.5-a, where an enlarged IBIC map (120 μm x 120 μm in size), obtained from the irradiation with 14.46 MeV Li ions of the diamond sample within the sensitive area of DBM, is reported. As for the Li ion beam IBIC map, similar structures are also visible in the IBIC map acquired for the other ion beams. This confirms a structural inhomogeneity of the detector's sensitive layer. In order to estimate the uniformity of the response, the distribution of the CCE in such irradiated area was analysed. For this purpose, the mean signal amplitude at each irradiated pixel was calculated and the standard deviation of the mean signal distribution provides a value of about 7 %, indicating a good degree of homogeneity of the detector response.

In order to investigate a correlation between the non-homogeneity regions and structural defects of diamond surface, the latter were measured using an atomic force microscope (AFM) in contact mode on face of the DBM. Fig.5-b displays a typical height image obtained over an area of 70 μm x 100 μm of the surface within the sensitive area of DBM. The surface comprises structural defects as parallel oriented scratches probably due to the mechanical polishing procedure of HPHT diamond substrate which are homoepitaxially reproduced in diamond layer during our CVD growth. Such scratches contribute the most to the surface roughness, whose average value is about 20 nm (*rms*) over 20 μm x 20 μm area. The stripe shape with low CCE, observed in IBIC map (see Fig.5-a), can be linked to these

superficial defects (see Fig.5-b). For this reason, the uniformity of the DBM response could be improved selecting a higher quality diamond substrate.

The normalized energy spectrum measured by DBM corresponding to the IBIC map of Fig.5-a is shown in Fig.6. The channels are converted to the energies applying the proper calibration described in the experimental section. The energy detected by DBM is about (0.295 ± 0.02) MeV. Lithium ion has sufficient energy to go through the detector (see Fig.3), depositing only a fraction of its incident kinetic energy inside the active diamond layer and resulting in a low amplitude signal.

The energy spectrum of the incident 14.46 MeV Li ions was simulated using Geant4 Monte Carlo simulation taking into account the structure of detector. The electronic noise of the entire experimental system has been also applied as a Gaussian distribution of σ=18 keV (experimentally estimated) to Monte Carlo simulation. The simulated spectrum is plotted as dot line in Fig.6. Good agreement was obtained between the simulated and experimental cases with 5 keV difference in peak position between two spectra. However, the experimental case exhibits a larger FWHM with respect to the simulated one and a tailing at the low-energetic areas on the left side of the energy peak. These discrepancies between two spectra can be mainly due to i) the inhomogeneity of the detector response and iii) an additional electronic noise under irradiation higher than the estimated one. The latter effect produce a symmetric broadening of the spectrum so that it is probably the most relevant source for the spectral broadening.

On the other hand, the small asymmetric distribution shape observed towards lower energies of the experimental spectrum is reasonably due to the inhomogeneity of the detector response. Indeed, the experimental energy spectrum can be well fitted by a double-Gaussian function. By applying a two-term Gaussian fit, it is possible to recognize a small peak (green gauss fit) at the low-energy part on the left side of the main peak (blue gauss fit). Such small peak is closed to the main peak but it is much more broadened. This is indicated in the energy spectrum as a tail towards lower energies. The two peaks can be described in terms of the inhomogeneity of the detector response. In particular, the main peak can be related to the particle impinging the high CCE regions of the detector (dark blue regions in IBIC map), while the second small peak to the ones hitting the low CCE regions (light blue regions). The areas ratio between the two Gaussian functions was about 7.3%, which is compatible with the homogeneity value of DBM reported above. Similar results have been obtained with the other ion beams used in this experiment.

The energies of all ions measured by DBM as a function of their calculated LET in diamond detector is reported in Fig.7. In order to calculate LET of different ions, Monte Carlo simulation was performed as described in experimental section. It is important to underline that the values of LET vary a bit within the thickness of the detector (about 0.8 μm) and therefore an average value of LET has been assumed and reported in Table 1. As clearly seen in Fig.7, a good linear behavior was observed and the linear correlation coefficient was found to be 0.998, as given by fitting experimental data with linear function. From the slope of the linear fit, a sensitive diamond thickness of about 0.70 ± 0.01 μm is derived, which is in excellent agreement with C-V measurement within the diamond surface roughness.

In order to preliminarily test the microdosimetric capabilities of the DBM and to assess the detector performances in relatively low LET radiation fields, it was irradiated with a 600 keV proton beam. A first spectrum was collected maintaining the detector face perpendicular to the beam axis. The energy spectrum is shown as thin continuous line in Fig.8-a. However, the energy peak is positioned very close

to the background electronic noise. In order to separate the signal yielded by protons from noise, the detector was tilted by an angle of 60° with respect to the beam axis. In this way, the path of the particles in the sensitive volume thickness is increased by a factor two i.e. 1.4 μm. The energy spectrum collected in this condition is shown as a thick continuous line in Fig.8-a. Both spectra are obtained collecting the signals of approximately 3500 particles.

The physical quantity of interest in microdosimetry is the lineal energy, y, which is a measure of the stochastic energy depositions along given chord length ($E/< l >$) [6]. For unidirectional irradiation and for this "slab" detector, the mean chord length of DBM, $< l >$, can be well approximated to the sensitive thickness of diamond on the basis of the detector geometry as evidenced in a previous theoretical study [16]. The diamond detector thickness at the two different tilting angles correspond to a water equivalent thickness of 2.46 μm (0°) and 4.93 μm (60°), respectively. The microdosimetric spectra obtained at the two different tilting angles are shown in Fig.8-b. Both spectra are normalized to unit dose. The spectrum collected with no tilting angle is truncated at low lineal energy values due to the electronic noise. The microdosimetric spectrum obtained at 0° tilting show a cutoff value of 32 keV/μm in lineal energy, whereas that obtained at 60° tilting show a complete spectrum with a lineal energy cutoff value of about 16 keV/μm. An increase in active volume thickness of diamond detector allows an increase in energy deposition so that complete microdosimetric spectra can be detected for low LET particles. However, different thicknesses of diamond detector may substantially modify the spectra shape. In particular, for thin detector and high particle energy, the range of the delta-rays may exceed the site size of detector and consequently part of the delta-rays energy may escape. On the contrary, for thick detector and low particle energy, the linear energy transfer of the particles can change significantly within the sensitive volume and the chance of the particle stopping within the sensitive volume can increase. In the framework of ion-beam therapy, i.e. proton and carbon beam, a large range of energies are used so that a suitable detector thickness should be chosen on the basis of the its application.

4. Conclusion

The fabrication and characterization of a novel design of diamond based detector, realized by combining both photolithography and selective growth CVD techniques, has been reported. Focused ion microbeam such as proton, helium, lithium, carbon and oxygen was used to investigate the properties of diamond based detector in view of microdosymetric applications in ion-beam therapy.

Measured IBIC maps have evidenced a well-defined confinement of the response within the active volume without any distortion of the signal due to welding material on the surface of diamond. The detector show a homogeneity of the CCE of about 7% over a large portion of the sensitive region. However, the sensitive region is characterised by regions of lower CCE appearing as thin parallel stripes. The IBIC map as well as the AFM inspection leads to the conclusion that such structural inhomogeneity are probably related to a polishing procedure of the diamond substrate so that they could be eliminated choosing a diamond substrate of higher quality.

The detector response shows a linear behavior as a function of the LET of the incident particle in the whole investigated LET range (from 100 – 3000 kev/μm) indicating that it could be used to detect a wide range of high energy particles as LET counter.

The preliminarily tests under irradiation from 600 keV protons showed how this diamond detector can be used for collecting microdosimetric spectra of lineal energy also in the framework of proton therapy which is today a challenge for solid-state microdosimeters. In this study, a lineal energy cutoff limit was identified at approximately 16 keV/μm for the proton path in water equivalent thickness of diamond. The lineal energies of 230-250 MeV proton (the highest proton energies used in hadron-therapy) decreases to values of the order of few keV/μm, emphasizing the need of further improvements i.e. increasing the sensitive volume thickness of the detector as well as decreasing the electronic noise.

As a general result, the agreement between the experimental results and Monte Carlo prediction provides insight about the physical behavior of the DBM, and together with their good performance observed during the experimental test, strengthens the possibility of using this detector ion-beam therapy microdosimetry applications. Work in progress in this direction.

Acknowledgment

This project has been partially supported by the H2020 project AIDA-2020, GA no. 654168. AIDA-2020-RBI-2016-01, user group leader Dr. Claudio Verona. Erasmus grant and the travel to the Ruđer Bošković Institute of one of the authors (M. Bandorf) was sponsored by Luca Tagliapietra with the company Helivertex .

Reference

[1] R. J. Nemanich, J. A. Carlisle, A. Hirata and K. Haenen, “CVD diamond- Research, Applications, and Challenges” , MRS Bullettin, Vol. 39, 490 (2014).

[2] Sussmann R.S., CVD diamond for Electronic Devices and Sensors (Wiley) 2009.

[3] M. Pillon, M. Angelone, G. Aielli, S. Almaviva, Marco Marinelli, E. Milani, G. Prestopino, A. Tucciarone, C. Verona, and G. Verona-Rinati, Journal of Applied Physics 104, 054513 (2008).

[4] J. A. Davis, S. Guatelli, M. Petasecca, M. L. F. Lerch, M. I. Reinhard, M. Zaider, J. Ziegler, and A. B. Rosenfeld, IEEE Transactions on Nuclear Science, 61, 4 (2014).

[5] R. R. Wilson, Radiobiology 47, (1946) 487-491.

[6] International Commission on Radiation Units and Measurements, Micordosimetry, ICRU report 36, Woodmont Avenue, Bethesda, Maryland, 20814, USA, 1983.

[7] J. A. Davis, K, Ganesan, A, D. C. Alves, D. A. Prokopovich, S. Guatelli, M. Petasecca, M. L. F. Lerch, D. N. Jamieson, and A. B. Rosenfeld, IEEE Transactions on Nuclear Science, 61, (2014) 3479-3484.

[8] J. A. Davis, K. Ganesan, D. A. Prokopovich, M. Petasecca, M. L. F. Lerch, D. N. Jamieson, and A. B. Rosenfeld, Appl. Phys. Lett. 110, 013503 (2017); doi: 10.1063/1.4973628.

[9] S. Rollet, M. Angelone, G. Magrin, M. Marinelli, E. Milani, M. Pillon, G. Prestopino, C. Verona, and G. Verona-Rinati, IEEE Transactions on Nuclear Science, 59 (2012).

[10] C. Verona, G. Magrin, P. Solevi, V. Grilj, M. Jakšić, R. Mayer, Marco Marinelli and G. Verona Rinati, J. Appl. Phys. 118, 184503 (2015).

[11] G. Magrin, R. Mayer, C. Verona, L. Grevillot, Radiat. Prot. Dosimetry, 166, 271-5 (2015) DOI: 10.1093/rpd/ncv175
[12] G. Sgouros et al J, Nucl Med 2010; 51:311–328. DOI: 10.2967/jnumed.108.058651
[13] J. Zhou et al, Cancer Management and Research, 7, 199–211 (2015) DOI: http://dx.doi.org/10.2147/CMAR.S46042
[14] I. Ciancaglioni, C. Di Venanzio, M. Marinelli, E. Milani, G. Prestopino, C. Verona, G. Verona-Rinati, M. Angelone, M. Pillon, and N. Tartoni, J. Appl. Phys. 110, 054513 (2011).
[15] T. Tadic´ and M. Jakšic, Nucl. Instr. Meth. B 267 (2009) 2028–2031.
[16] P. Solevi, G. Magrin, D. Moro and R. Mayer, Phys. Med. Biol., 60, 7069 (2015) DOI: https://doi.org/10.1088/0031-9155/60/18/7069
[17] S Agostinelli et al, Nucl. Instrum. Meth. A, 506, 250-303 (2003) DOI: https://doi.org/10.1016/S0168-9002(03)01368-8
[18] M. Jakšić, I. Bogdanović Radović, M. Bogovac, V. Desnica, S. Fazinić, M. Karlušić, Z. Medunić, H. Muto, Ž. Pastuović, Z. Siketić, N. Skukan and T. Tadić, Nucl. Instrum. Methods Phys. Res. B 260 (2007) 114–118.

Table 1 – Monte Carlo calculated penetration depths in diamond and average LET in a 0.8 μm diamond layer for all the employed ions.

Ion type	Ion Energy (MeV)	Penetration depth in diamond (μm)	LET@0.8μm diamond (KeV/ μm)
^{1}H	0.6	3.7	116
^{4}He	5.47	14.3	258
^{7}Li	1.6	1.8	1096
^{7}Li	6.4	7.8	669
^{7}Li	14.46	21.1	412
^{12}C	3.75	2	2500
^{12}C	8.43	4.1	2195
^{12}C	15.00	7.5	1794
^{12}C	23.43	13	1460
^{16}O	17.58	6.2	2870

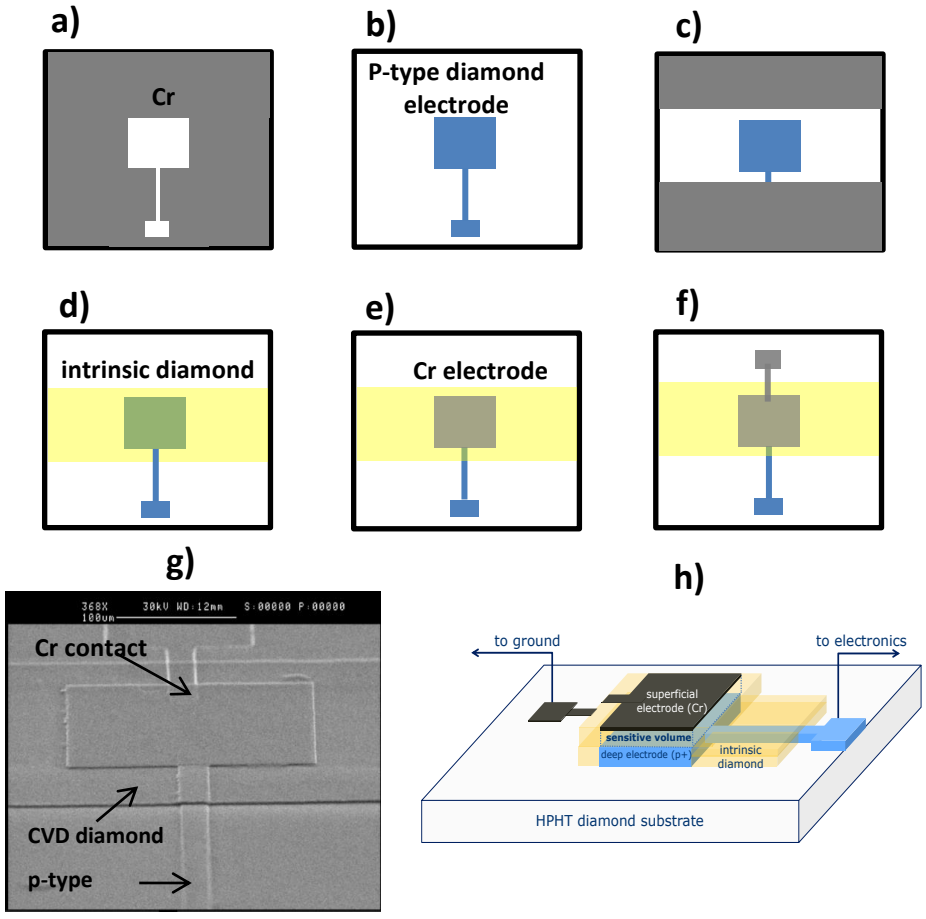

Fig.1 Main steps of the fabrication process of diamond based microdosimeter: a) First deposition of a patterned Cr plasma-resistant mask , b) selective growth of p-type diamond (back electrode), c) second deposition of a patterned Cr mask, d) selective growth of intrinsic diamond (sensitive layer), e) deposition of Cr top electrode, and f) realization of the bond pad electrode. g) SEM image and h) schematic representation of the DBM.

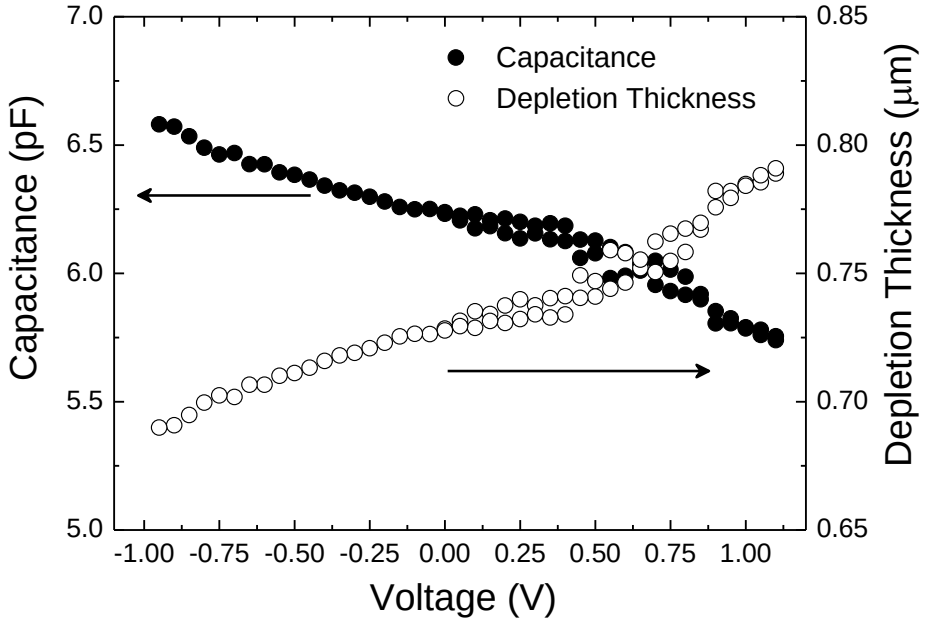

Fig.2 Capacitance-Voltage characteristic and corresponding depletion thickness of DBM.

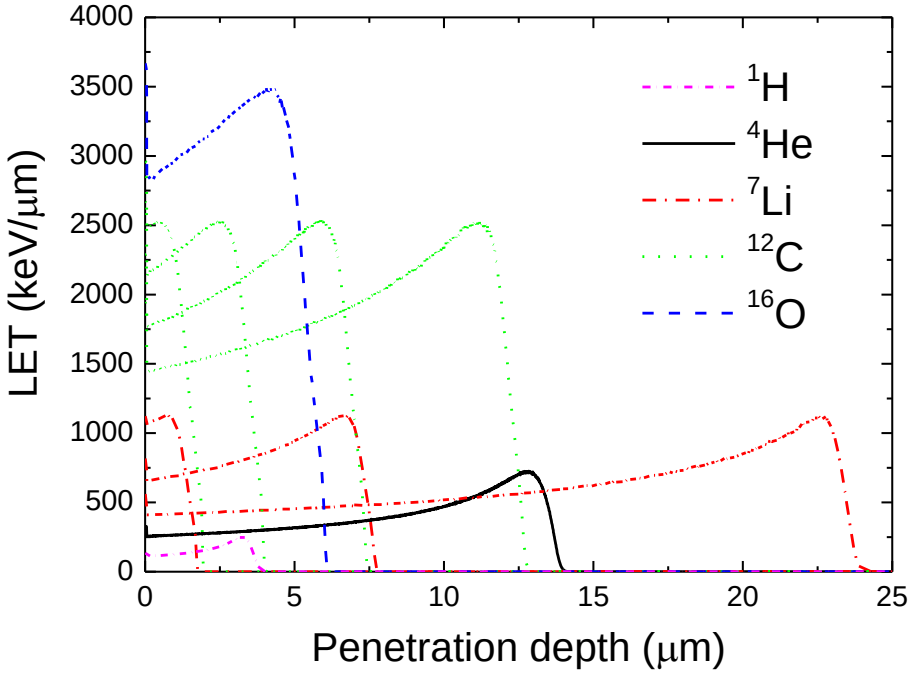

Fig.3 Simulated curve based on Geant4 Monte Carlo calculation of ions LET in diamond detector. Chromium contact was also included in the Monte Carlo simulation.

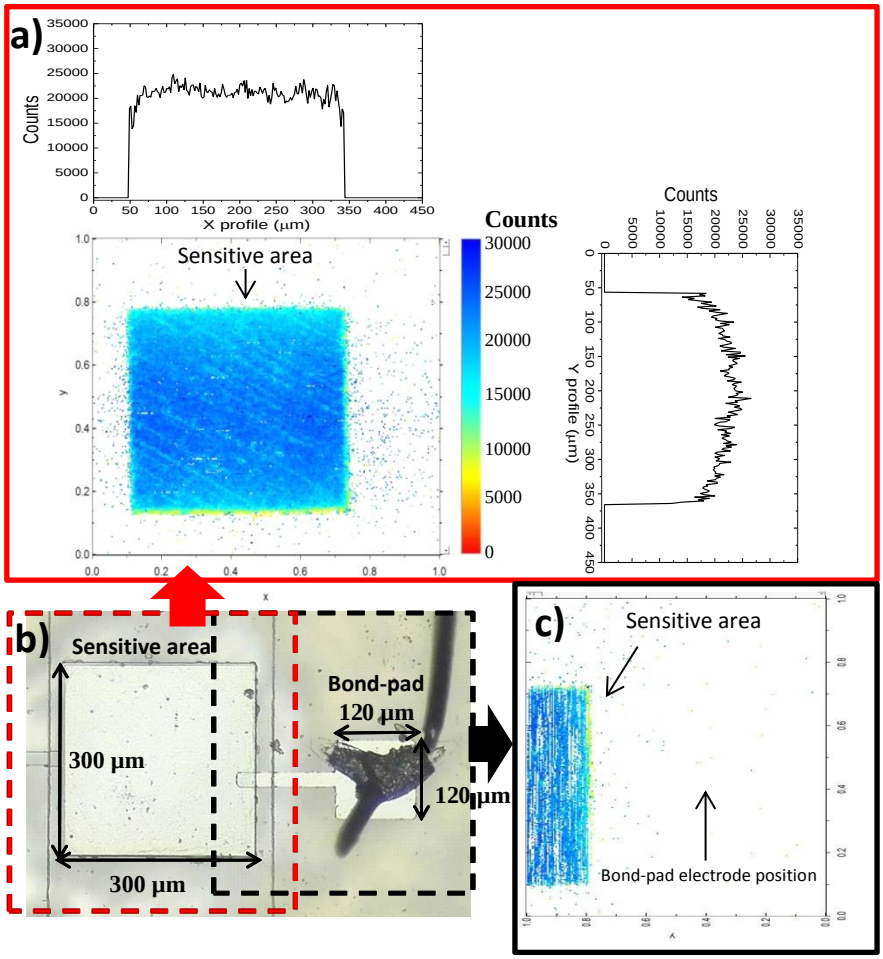

Fig.4 Typical IBIC pulse height 2D distributions measured over both the whole sensitive square area (a) and near to the bond pad (c) of DBM. Optical image of DBM is reported as a guide for the eye (b). The X and Y profiles of the sensitive square area are also shown.

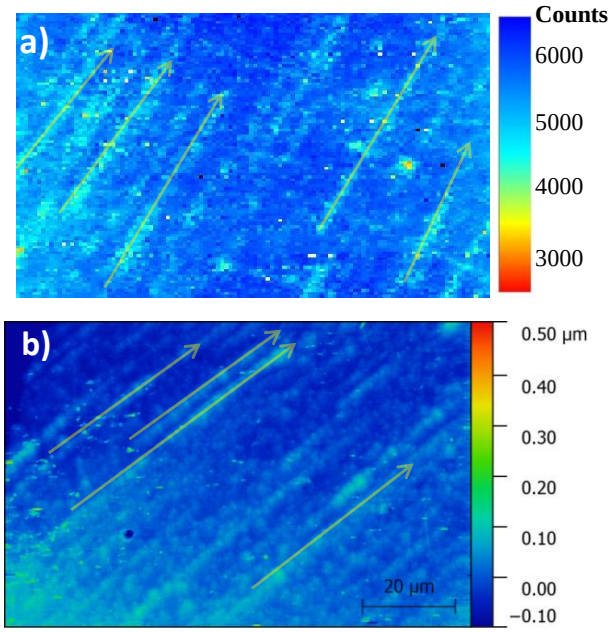

Fig.5 a) IBIC map (120 µm x 120 µm in size) obtained from the irradiation with 14.46 MeV Li ions of the diamond sample within the sensitive area. b) Typical AFM image obtained over an area of 70 µm x 100 µm of the diamond surface positioned inside of the chromium superficial electrode.

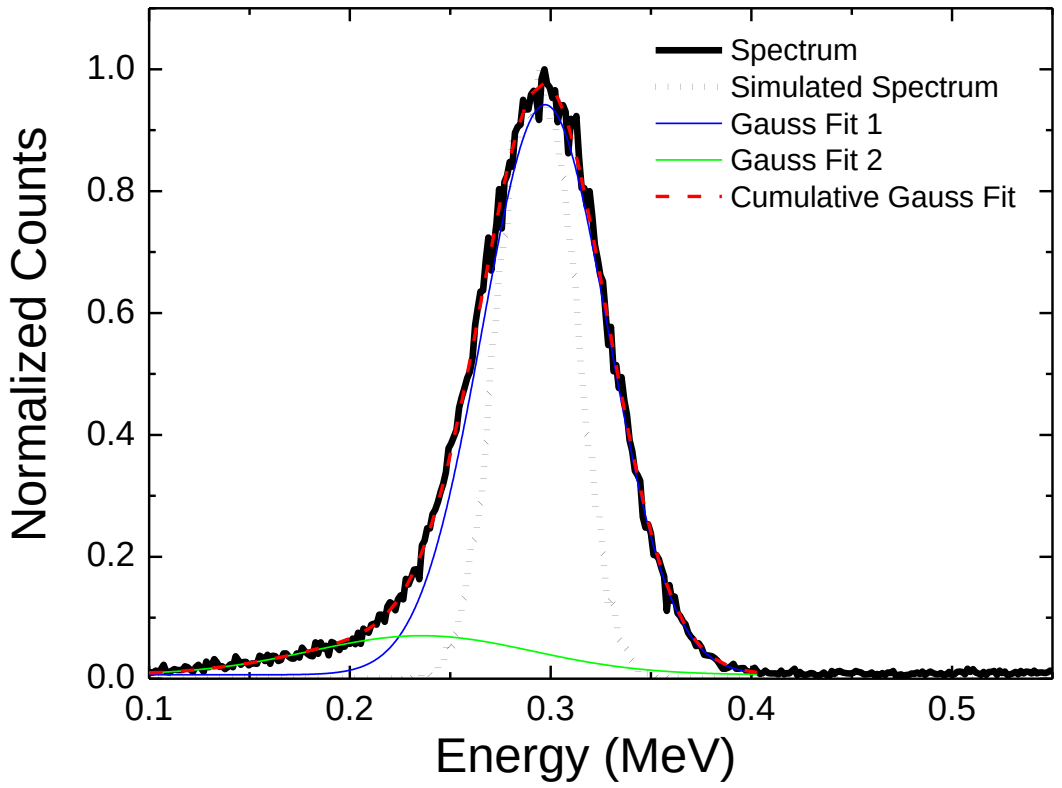

Fig.6 Normalized energy spectra measured by DBM for 14.46 MeV Li ions and simulated by Geant4 Monte Carlo. Double-Gaussian fit is also reported in figure.

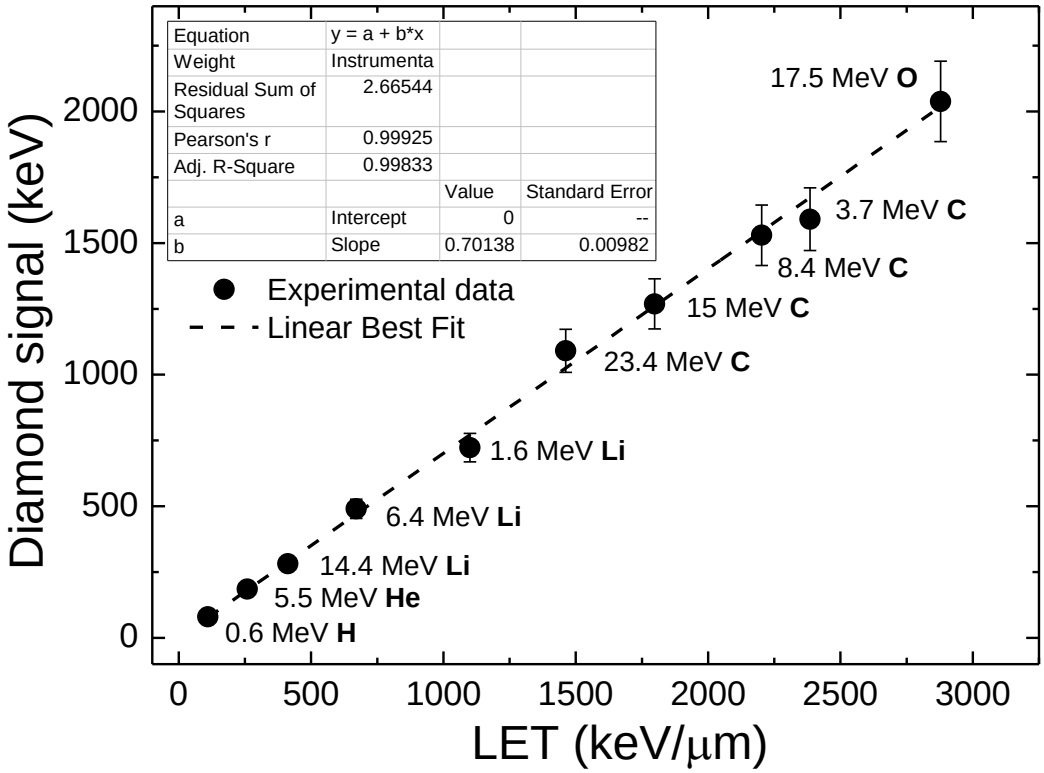

Fig.7 The energy measured by DBM as a function of the LET of the ions used in the experiment. Linear fit of the experimental data is also reported in the figure as dashed line.

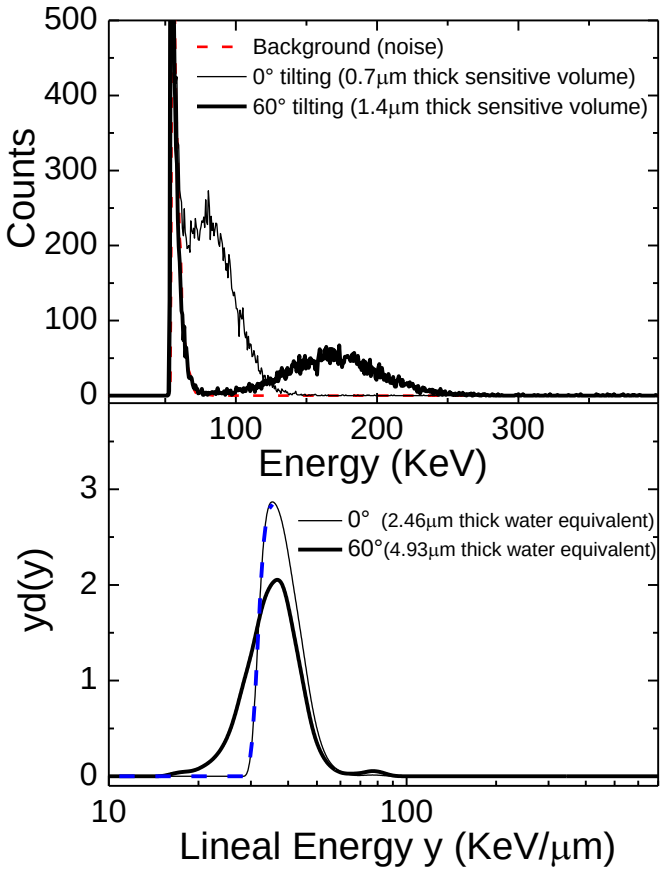

Fig. 8. a) Energy spectra of 600keV $^{1}H^{+}$ collected orientating the detector surface normal to the beam direction and for tilting the detector surface by 60° toward the beam direction. b) Microdosimetric spectra of 600keV protons obtained with DBM at the two conditions. The two microdosimetric spectra referred to diamond at liquid water density (1 g·cm^{-3}). The spectrum at 0° is voluntarily truncated due to the electronic noise.